Modeling and Control Design of a Wind Tunnel Model Support

David A. Howe

November 1990

NASA

National Aeronautics and
Space Administration

Modeling and Control Design of a Wind Tunnel Model Support

David A. Howe, Ames Research Center, Moffett Field, California

November 1990

NASA

National Aeronautics and
Space Administration

Ames Research Center
Moffett Field, California 94035-1000
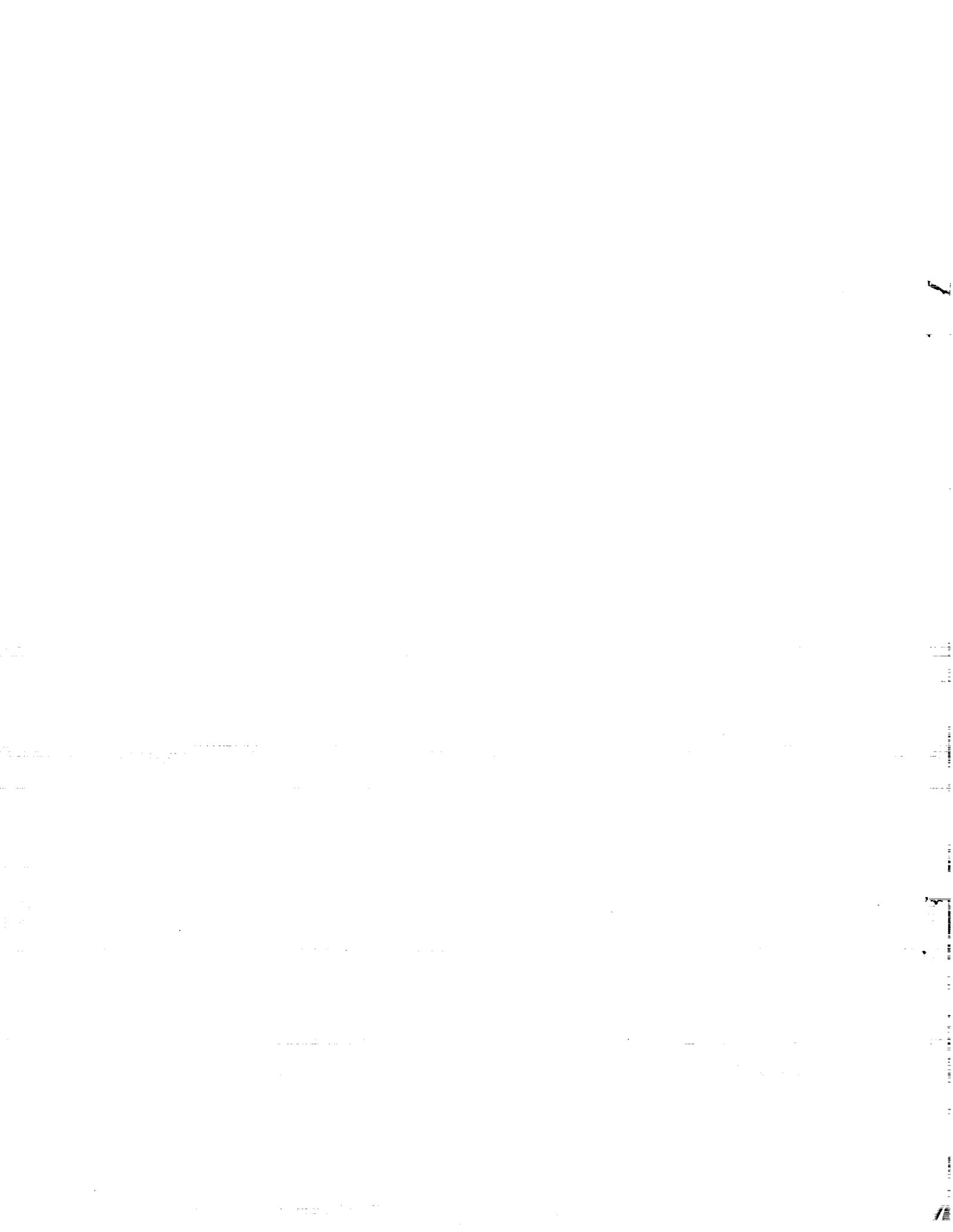
MODELING AND CONTROL DESIGN OF A WIND TUNNEL MODEL SUPPORT

David A. Howe
Control Systems Engineer
NASA Ames Research Center
Moffett Field, California, USA

ABSTRACT

The 12-Foot Pressure Wind Tunnel at Ames Research Center is being restored. A major part of the restoration is the complete redesign of the aircraft model supports and their associated control systems. An accurate trajectory control servo system capable of positioning a model (with no measurable overshoot) is needed. Extremely small errors in scaled-model pitch angle can increase airline fuel costs for the final aircraft configuration by millions of dollars. In order to make a mechanism sufficiently accurate in pitch, a detailed structural and control-system model must be created and then simulated on a digital computer. The model must contain linear representations of the mechanical system, including masses, springs, and damping in order to determine system modes. Electrical components, both analog and digital, linear and nonlinear must also be simulated. The model of the entire closed-loop system must then be tuned to control the modes of the flexible model-support structure. The development of a system model, the control modal analysis, and the control-system design are discussed.

NOMENCLATURE

K_t motor torque constant, in. lb/A

R_{tt} terminal-to-terminal motor winding resistance, ohms

s the Laplace operator (represents the derivative with respect to time)

T_e motor electrical time-constant, sec

T_m motor mechanical time-constant, sec

z control-system damping ratio

θ rotational angle, deg (rad)

$\dot{\theta}$ derivative of θ with respect to time, deg/sec (rad/sec)

INTRODUCTION

The 12-Foot Pressure Wind Tunnel is one of some 30 research wind tunnels at Ames Research Center. These tunnels are used for research by numerous aircraft companies, as well as by many governmental agencies. The 12-ft tunnel [test section 12 ft (3.66 m) in diameter] is a closed-circuit wind tunnel with air flow provided by a 15,000-hp fan-drive system. Since the 12-ft is only capable of speeds less than Mach 0.6, it is used primarily for takeoff, landing, and slow maneuver studies.

The rear strut support (RSS) is the most frequently used support in the wind tunnel. Models with average wingspans of about 6 ft (1.88 m) and weighing less than 600 lb (273 kg) can be tested on the rear strut. The RSS consists of a large, vertically moving strut with a pitch/roll mechanism attached at the centerline. A massive steel sting extends from the roll drive into the back end of the model (Fig. 1). The model is pitched and rolled to achieve the aerodynamic angles of pitch (α) and sideslip (β), while the strut is driven vertically (heave) to maintain the model on tunnel centerline. The accuracy of the pitch angle is very important since small errors can cause large increases in drag. Additionally, overshoot cannot be tolerated because of aerodynamic hysteresis. Previous model-support control systems in the tunnel have used open-loop pitch control that had very poor repeatability and high settling times. The restoration of the 12-ft tunnel has allowed us to correct this inadequacy. The new control system will be capable of accurate trajectory control ($\pm0.05°$ (0.0008727 rad) throughout an entire move). It will be accurate to $\pm0.01°$ (0.0001745 rad) at the endpoint with no measurable overshoot. The model support will slew at a rate up to 1°/sec (0.01745 rad/sec).

The high aerodynamic loads on the wind-tunnel model necessitate a powerful prime mover and very high gear ratios in the pitch-drive system. Details of the prime-mover selection will not be discussed in this paper; however, a brushless dc electric motor provided the best power for its physical size. The emphasis in this discussion will be on control-system modeling and design of the model pitch system. Since the pitch degree-of-freedom is the most dynamically active, it provides great insight into the behavior of the entire system. The discussion that follows includes control theory and mathematical-device modeling, followed by appropriate Bode and root locus plots to demonstrate system performance and system mode control. Final system performance will be presented in a time-response plot. The design was accomplished using a digital-control-system analysis package in which each of the system components was represented by a mathematical model, or transfer function, given in the complex frequency domain.

SYSTEM MODELING

To study the dynamic performance of the mechanism and to develop a servo control system, a model representing the physical components of the system was created. This model included electrical components such as the transducers, the motion controllers (both analog and digital), and the software routines contained within the digital controller. The mechanical system was modeled to included masses, springs, and dampers. Nonlinear system components such as limiters were also included. Finally, the electrical properties of the motor and its amplifier were modeled. The entire system model is shown in Figure 2, and will be referred to in the discussion of the modeling and control-system design.

STRUCTURE

Figure 3 shows the mechanical structure model of the pitch mechanism and its mathematical representation is shown in Figure 2a. The model was simplified by assuming that the structure behaved as a three-inertia (mass) system. Two structural members in the mechanism were known to be weak; thus, a three-inertia system was a good representation of the entire system. Reflecting the components back to the prime mover (motor) allowed us to solve for the transfer functions defining the equations of motion:

$$\frac{\text{Inertia 3 Position}}{\text{Input Torque}} = \frac{\theta_3}{T_{ls}}$$

$$= \frac{1.36 \times 10^{-8}}{S^2} \times \frac{\left\{ \begin{array}{l} \left[S^2 + 2(0.05)(57.5)S + (57.5)^2\right] \\ \times \left[S^2 + 2(0.05)(565)S + (565)^2\right] \end{array} \right\}}{\left\{ \begin{array}{l} \left[S^2 + 2(0.05)(57.5)S + (57.5)^2\right] \\ \times \left[S^2 + 2(0.05)(565)S + (565)^2\right] \end{array} \right\}} \quad (1)$$

$$\frac{\text{Inertia 2 Position}}{\text{Input Torque}} = \frac{\theta_2}{T_{ls}}$$

$$= \frac{4.54 \times 10^{-7}}{S^2} \times \frac{\left\{ \begin{array}{l} (S+9200) \\ \times \left[S^2 + 2(0.05)(57.5)S + (57.5)^2\right] \end{array} \right\}}{\left\{ \begin{array}{l} \left[S^2 + 2(0.05)(57.5)S + (57.5)^2\right] \\ \times \left[S^2 + 2(0.05)(565)S + (565)^2\right] \end{array} \right\}} \quad (2)$$

$$\frac{\text{Inertia 1 Position}}{\text{Input Torque}} = \frac{\theta_1}{T_{ls}}$$

$$= \frac{2.97 \times 10^{-6}}{S^2} \times \frac{(S+526) \times (S+9200)}{\left\{ \begin{array}{l} \left[S^2 + 2(0.05)(57.5)S + (57.5)^2\right] \\ \times \left[S^2 + 2(0.05)(565)S + (565)^2\right] \end{array} \right\}} \quad (3)$$

Notice that the structure has modes at 57.5 and 565 rad/sec with 0.05 damping. These modes will be kept stable by including a velocity loop around the motor. The zeros in the structure, although at high frequency, will aid in damping. The total combined structure transfer function was defined as θ_1/T_{ls}.

MOTOR DRIVE SYSTEM

The motor and gearbox were then be added to the system model (Figs. 2b, 2c). The motor was modeled as a second-order system with one pole defined by the electrical time-constant and the other by the mechanical time-constant. There is a gain associated with this transfer function which is the product of terminal-to-terminal conductance and the motor torque constant. The electrical and mechanical system poles were separated in the model so that motor current could be fed back to the inner current loop. The separate transfer functions are shown below.

$$\frac{\text{Motor torque}}{\text{Motor current}} = \frac{K_t}{[1 + T_m(S)]}$$

where

$$K_t = 9.74 \text{ (in.-lb/A)}$$

$$T_m = 1.92 \times 10^{-3} \text{ (sec)}$$

and

$$\frac{\text{Motor current}}{\text{Motor voltage}} = \frac{1/R_{tt}}{[1 + T_e(S)]}$$

where

$$1/R_{tt} = 0.45 \text{ (mho)}$$

$$T_e = 13.35 \times 10^{-3} \text{ (sec)}$$

The gearbox becomes a simple gain term in the model. Since the gear ratio is 15,330/1, the motor behaves as if it were running unloaded.

As can be seen above, the motor adds two real poles, one at 521 rad/sec and another at 74.9 rad/sec. The low-frequency motor pole will need to be pushed to a much higher frequency to avoid exciting the mode of the structure located at 57.5 rad/sec. The current loop will be used to move this pole out to a higher frequency.

Additionally, there is a back-EMF produced by the motor which must be included in the model. This back-EMF is a voltage that is proportional to motor speed, but whose polarity is opposite that of the applied voltage. The overall effect of the back-EMF is to limit the current flowing through the motor by limiting the applied voltage.

2

CONTROLLERS

A digital controller (Fig. 2e) was used to control the pitch mechanism position, and an analog controller (Fig. 2d) was used to control motor velocity and current. The model-support pitch mechanism is commanded with a quadratic position profile (trapezoidal velocity profile) which must be generated by the digital controller. The digital controller must also contain an equivalent summing junction in order to compute position error. The controller will be a distributed-control-system (DCS) processor that contains a PID (proportional-integral-derivative) algorithm with velocity feedforward. All of these features, including the controller update time, must be included in the system model. With these algorithms available in the controller, it should be possible to tune the system to control the natural oscillation modes of the structure.

The velocity controller, within the motor amplifier, receives its command from the position controller. This controller contains an analog summing junction as well as compensation. A lead/lag compensator and an integrator are included within this loop. The integrator forces the velocity loop to track the input, and the compensator allows system performance to be further improved. The mathematical model of this controller was also included in the control-system model.

The final controller within the motor amplifier is the current controller (Fig. 2c). This controller gets its command from the velocity controller in the form of a current command. The mathematical model of this controller was simply a gain and two summing junctions. The first summing junction was used to compute current error (commanded current minus actual current), and the second was used to simulate the effect of the back-EMF by reducing available motor armature voltage. The gain was adjusted to push the motor's natural poles out to higher frequencies so that the structure's lightly damped modes would not be adversely affected.

The final elements in the system model were feedback transducers. There are velocity and position transducers in the system. These transducers are not located in the same place; the advantage of this "non-colocation" will be discussed later. Both of these transducers are resolvers, and they have a better response time than the rest of the system. Also, both of these transducers were modeled as simple gains since their high-frequency dynamics do not affect system performance.

CONTROL ANALYSIS AND DESIGN

To begin the control-system analysis and design, the innermost loop was tuned with all the other loops open. Then each loop was closed and tuned concentrically, until all the control loops were closed and tuned. This tuning process took place with only the linear and continuous model blocks in place. By eliminating the nonlinear and discrete control blocks, classical methods of control-system design could be used. Only after the linear system was tuned, could the nonlinear blocks and discrete blocks be added to the model and their effects studied. The addition of these nonlinearities may upset the "tuned" system, and readjustment of the compensation may be required.

This discussion begins with the open-loop motor and structure blocks of the system model. The theoretical zeros and poles of the system are shown in Table 1.

Table 1. Open-loop motor and structure zeros and poles.

	Eigenvalues	Frequency, rad/sec	Damping, z
Zeros			
Structure	-526	526	
Structure	-9200	9200	
Poles			
Structure	$-3.0 \pm j57.4$	57.5	0.05
Structure	$-29.6 \pm j565$	565.0	0.05
Structure			
Acceleration integrator	0	0	
Velocity integrator	0	0	
Motor	-74.9	74.9	
Motor	-521	521	

The structure poles are lightly damped, whereas the motor poles are real and thus highly damped. Notice that the low-frequency motor pole is very close to the low-frequency structure pole. This will cause the structural mode at 57.5 rad/sec to be excited, and the mechanism will oscillate owing to the light damping on the structure poles. The open-loop Bode plot of this system is shown in Figure 4.

The next step was to close the current loop (including back-EMF). The Bode plot is shown in Figure 5, and the new system roots are shown in Table 2.

Table 2. Current-loop zeros and poles.

	Eigenvalues	Frequency, rad/sec	Damping, z
Zeros			
Structure	-526	526	
Structure	-9200	9200	
Poles			
Structure	$-3.0 \pm j57.4$	57.5	0.05
Structure	$-29.6 \pm j565$	565.0	0.05
Structure			
Acceleration integrator	0	0	
Velocity integrator	0	0	
Motor	-520	520	
Motor	-2856	2856	

As can be seen in the Bode plot, closing the current loop has added phase margin to the system which will aid in closing subsequent loops. The structure poles did not move, but the low-frequency motor pole moved to a much higher frequency.

3

With the current loop in place, the interaction between the open-loop motor pole and the low-frequency structure pole can be avoided, and the system will oscillate at an acceptably high frequency.

The velocity loop was the next loop to be closed. This loop will force the motor to track the velocity command. To choose an appropriate velocity loop gain, a root locus was created to track the pole locations as a function of loop gain. The velocity loop gain was then increased to enhance the frequency response of the system and to force the system to have a damping ratio of 0.7. The root locus, with the resultant root locations identified, is shown in Figure 6.

A feedback gain for the velocity transducer was chosen; the resultant roots for the system are shown in Table 3.

Table 3. Velocity-loop zeros and poles.

	Eigenvalues	Frequency, rad/sec	Damping, z
Zeros			
Structure	$-3.0 \pm j57.4$	57.5	0.05
Structure	$-29.6 \pm j565$	565.0	0.05
Velocity compensation	20	20	
Poles			
Structure	$-3.0 \pm j57.4$	57.5	0.05
Structure	$-29.6 \pm j565$	565.0	0.05
Structure			
Acceleration integrator	-23.1	23.1	
Velocity integrator	0	0	
Motor	-3005	3005	
Motor	$-175 + j181$	252	0.7
Velocity compensation	$-175 - j181$	252	0.7
Velocity compensation	$-2060 \pm j542$	2130	0.97

The velocity loop compensation available within the controller is limited. There is a fixed lag at 2100 rad/sec and a lead with variable frequency (the zero can be placed at 10 rad/sec or higher). A zero was chosen to be at 20 rad/sec and the pole was placed at 2020 rad/sec to give the best overall response. The Bode plot is shown in Figure 7. As can be seen in the system model, the position and velocity transducers are placed in two different locations.

The difference in the locations of the transducers can be explained by looking at the transfer function, θ_3/T_{ls}. This transfer function has two zero pairs in the numerator of the transfer function. These zeros, enclosed within the velocity loop, tend to keep the structure poles from moving into the right-hand plane and becoming unstable. Because these poles are held in place, the velocity gain can be increased to achieve the desired system response and force the device to track the velocity

command. If the velocity transducer had been placed on the load, the zeros would have cancelled out, and the structure poles would not have been restrained to the left-half plane. The velocity transducer was thus placed on the motor in the velocity feedback loop, and the position transducer was placed on the load (θ_2) to ensure that the final position matches the position setpoint.

The final loop to be closed was the position loop. This loop was closed with a digital controller by using a proportional-integral-derivative (PID) algorithm and velocity feedforward. The system model was first tuned by using the continuous system model with a proportional-only controller. The position loop gain was chosen to give the best dynamic response. The root locus of the system is shown in Figure 8.

The resultant roots are shown in Table 4.

Table 4. Position-loop zeros and poles.

	Eigenvalues	Frequency, rad/sec	Damping, z
Zeros			
Structure	$-3.0 \pm j57.4$	57.5	0.05
Structure	$-29.6 \pm j565$	565.0	0.05
Velocity compensation	20	20	
Poles			
Structure	$-2.9 \pm j57.4$	57.5	0.05
Structure	$-30.2 \pm j565$	565.0	0.05
Structure			
Acceleration integrator	-24.5	24.5	
Velocity integrator	-5.73	5.73	
Motor	-3005	3005	
Motor	$-171 + j176$	245	0.7
Velocity compensation	$-175 - j176$	245	0.7
Velocity compensation	$-2059 \pm j542$	2130	0.97

The low-frequency structure pole became slightly less damped, and the high-frequency structure pole became slightly more damped. These two pole-pairs moved very little, a result of the velocity transducer placement on the motor. The motor electrical and the velocity compensator pole-pair moved more toward critical damping and decreased slightly in frequency. The velocity integrator moved out in frequency to 5.73 rad/sec, becoming the dominant pole and thus limiting the frequency response of the system to about 0.9 Hz. The Bode plot of the position loop is shown in Figure 9.

The next step in tuning the system was to include the computer update time and the PID and velocity feedforward algorithms. The system response was optimized for a quadratic position profile (trapezoidal velocity profile) input since this is the setpoint trajectory the model support must follow. The system

worked best with a combination of proportional gain, derivative gain, and velocity feedforward. Finally, the nonlinear elements were added to the model. There were saturation blocks for motor current and voltage, as well as a switch to simulate the digital position loop controller. The model was then retuned with all the elements in place. It was found that a digital position loop controller running at 10 Hz was capable of controlling the trajectory of the model support within 0.03° (0.000523 rad) and limit the overshoot to 0.007° (0.000122 rad), as shown in Figure 10. These two performance figures are within our design specifications and the 10-Hz loop rate will be achievable with all common distributed control systems.

CONCLUSION

A detailed system model of the model-support control system has demonstrated that the design parameters of trajectory control to ±0.05° (0.0008727 rad) throughout an entire move and an accuracy of ±0.01° (0.0001745 rad) at the endpoint with no measurable overshoot are theoretically achievable. The model has shown that by careful placement of feedback transducers and proper control-system tuning, a very lightly damped structure can be kept stable despite its natural tendency to go unstable. It has been found that the natural oscillating modes of devices such as motors can be significantly altered through the use of feedback. Such a model is very valuable in identifying lightly damped structural modes and allows a control systems engineer to design compensation before actual device construction.

## ACKNOWLEDGMENTS
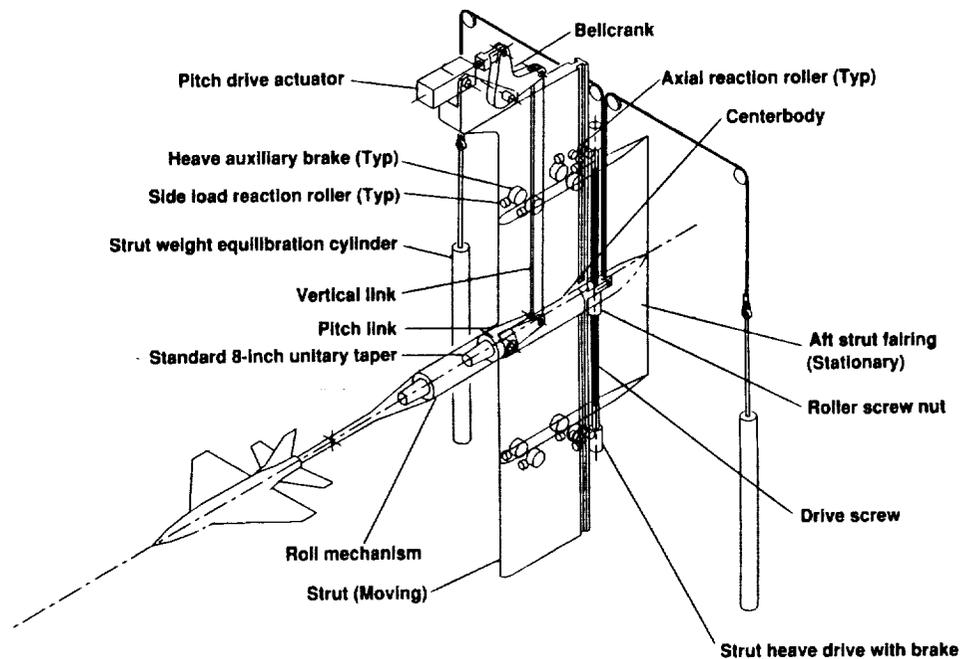
Figure 1. RSS model support.

5
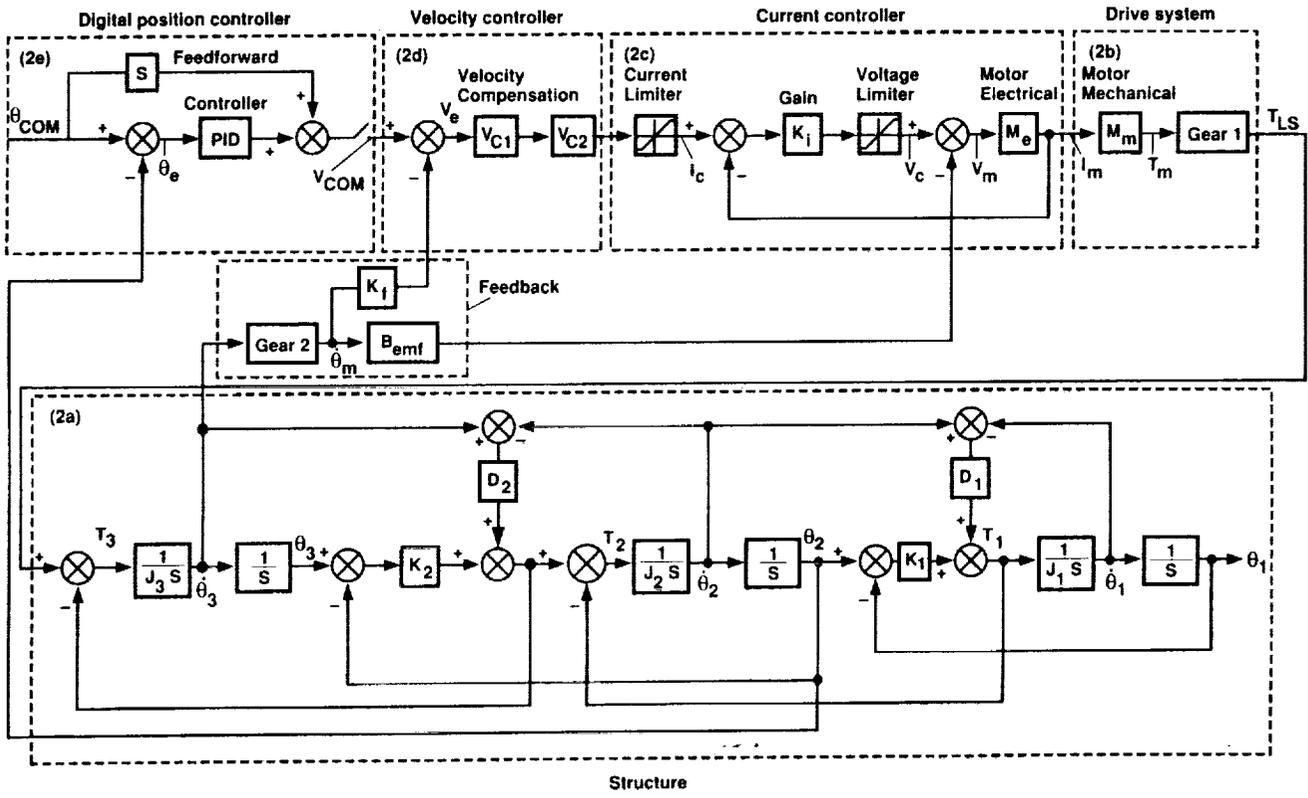
Figure 2. Control-system model.
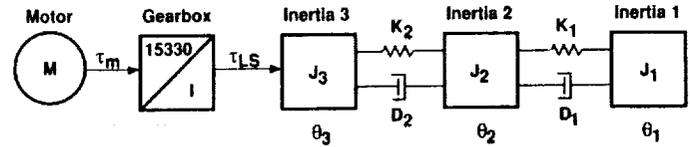
Figure 3. Mechanical structure model.
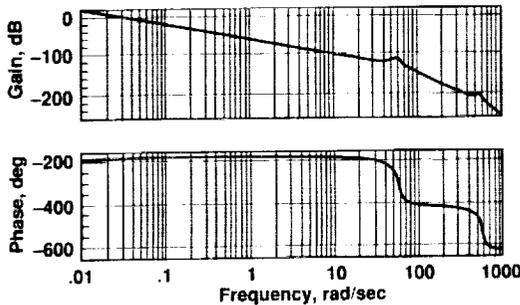
Figure 4. Bode plot of open-loop motor and structure (θ_1/V_m).
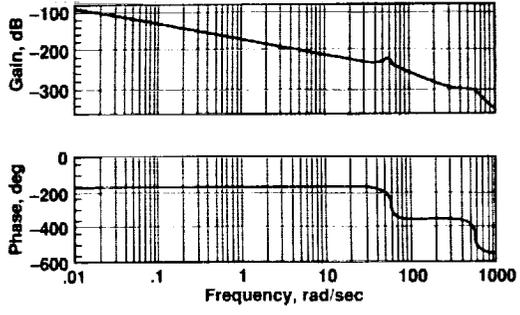

Figure 5. Bode plot of current loop with back-EMF (θ_1/I_c).

6
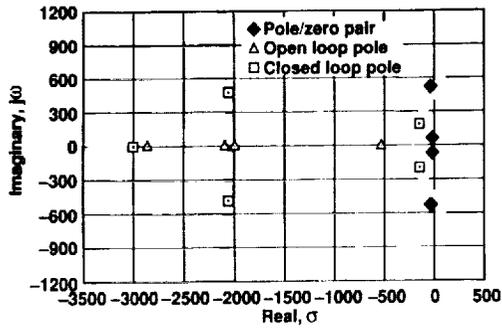
Figure 6. Root locus of velocity feedback gains.
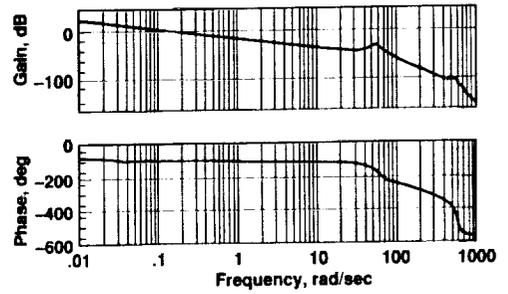

Figure 9. Bode plot of position feedback loop (θ_1/θ_{com}).
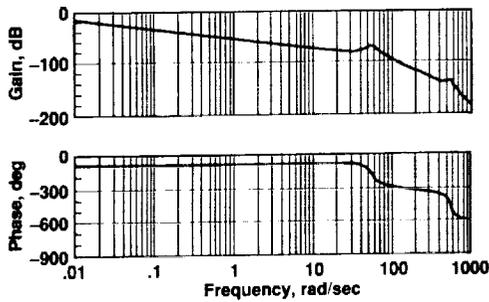
Figure 7. Bode plot of velocity feedback loop (θ_1/V_{com}).
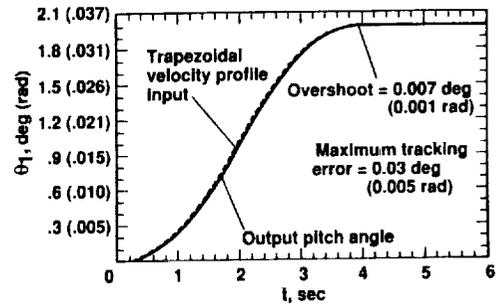
Figure 10. System position time-response (θ_1/θ_{com}).
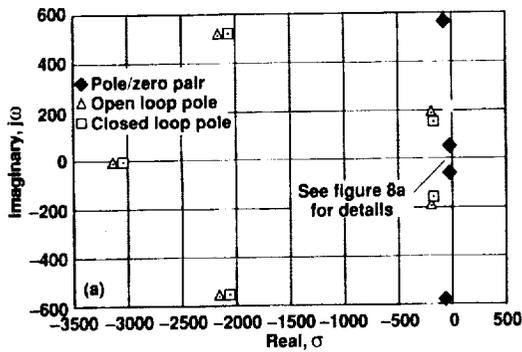
Figure 8a. Root locus of position feedback gains.
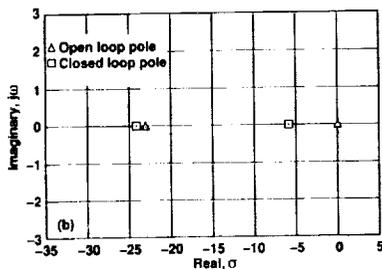
Figure 8b. Root locus of position feedback gains (near zero).

NASA
National Aeronautics and
Space Administration

Report Documentation Page

1. Report No. NASA TM-103829	2. Government Accession No.	3. Recipient's Catalog No.

4. Title and Subtitle	
Modeling and Control Design of a Wind Tunnel Model Support	5. Report Date November 1990
	6. Performing Organization Code

7. Author(s)	8. Performing Organization Report No.
David A. Howe	A-91008
	10. Work Unit No. 2189

9. Performing Organization Name and Address	11. Contract or Grant No.
Ames Research Center Moffett Field, CA 94035-1000	
	13. Type of Report and Period Covered Technical Memorandum

12. Sponsoring Agency Name and Address	
National Aeronautics and Space Administration Washington, DC 20546-0001	14. Sponsoring Agency Code

16. Abstract

The 12-Foot Pressure Wind Tunnel at Ames Research Center is being restored. A major part of the restoration is the complete redesign of the aircraft model supports and their associated control systems. An accurate trajectory control servo system capable of positioning a model (with no measurable overshoot) is needed. Extremely small errors in scaled-model pitch angle can increase airline fuel costs for the final aircraft configuration by millions of dollars. In order to make a mechanism sufficiently accurate in pitch, a detailed structural and control-system model must be created and then simulated on a digital computer. The model must contain linear representations of the mechanical system, including masses, springs, and damping in order to determine system modes. Electrical components, both analog and digital, linear and nonlinear must also be simulated. The model of the entire closed-loop system must then be tuned to control the modes of the flexible model-support structure. The development of a system model, the control modal analysis, and the control-system design are discussed.

17. Key Words (Suggested by Author(s))	18. Distribution Statement
Wind tunnel Model support Controls simulation Control system	Unclassified-Unlimited Subject Category - 33

19. Security Classif. (of this report)	20. Security Classif. (of this page)	21. No. of Pages	22. Price
Unclassified	Unclassified	8	A02